SAND2022-8315C

2022 International High-Level Radioactive Waste Management Conference

DECOVALEX Task F DOE Crystalline Reference Case Results

Rosie Leone*, Emily Stein*, and Jeffrey D. Hyman**

*Sandia National Laboratories, P.O. Box 5800, Albuquerque, NM 87123 USA, rleone@sandia.gov
** Los Alamos National Laboratory, P.O. Box 1663, Los Alamos, NM 87545 USA, jhyman@lanl.gov

Performance assessment is an important tool to estimate the long-term safety for a nuclear waste repository. Performance assessment simulations are subject to multiple kinds of uncertainty including stochastic uncertainty, state of knowledge uncertainty, and model uncertainty. Task F1 of the DECOVALEX project involves comparison of the models and methods used in post-closure performance assessment of deep geologic repositories in fractured crystalline rock, providing an opportunity to compare the effects of different sources of uncertainty. A generic reference case for a mined repository in fractured crystalline rock was put together by participating teams, where each team was responsible for determining how best to represent and implement the model. This work presents the preliminary crystalline reference case results for the Department of Energy (DOE) team.

I. INTRODUCTION

DECOVALEX stands for the DEvolopment of COupled models and their VALidation against Experiments. DECOVALEX is an international research project comprising participants from industry, government, and academia, focusing on development of understanding, models and codes in complex coupled problems in sub-surface geological and engineering applications; DECOVALEX-2023 is the current phase of the project. Task F of DECOVALEX-2023 is a comparison of the models and methods used in post-closure performance assessment of deep geologic repositories. In Task F1, the system for comparison is a generic repository for commercial spent nuclear fuel (SNF) in a fractured crystalline host rock. Participating teams agreed on a common description of the features, events, and processes to be considered in the initial reference case, and to quantitatively characterize and parameterize associated materials and models using values from the literature.

The Task F1 preliminary reference case for a mined repository in fractured crystalline rock is defined in the DECOVALEX Task F Specification [11]. The preliminary reference case assumes steady state flow and transient transport of two conservative tracers upon simultaneous breach of all the canisters in the repository. Teams will run the simulation on ten different stochastic fracture realizations and compare tracer transport and steady state flow across the top surface of the model domain. The results of Task F will help build confidence in the models, methods, and software used for post-closure performance assessment, and/or to bring to the fore additional research and development needed to improve performance assessment methodologies.

This paper presents the work done by Sandia National Laboratories and Los Alamos National Laboratory for the U.S. Department of Energy (DOE) team. Section II describes an overview of the generic crystalline repository, Section III discusses the methods used by the DOE team, Section IV describes the output metrics for comparison, and Section V presents preliminary results.

II. GENERIC CRYSTALLINE REPOSITORY

II.A. Geological Setting

The reference case repository is located beneath a gently sloping hill in a domain 5 km in length, 2 km in width, and ~1 km in depth (Fig. 1). The repository is located in the west (left) side of the domain, and the area of lowest elevation is located on the east (right) side of the domain. Surface elevation decreases 20 m over a distance of 2 km; the hydraulic pressure at the top surface of the domain is used to mimic the topography. Conceptually, the area of lowest elevation represents the location where water would collect at the surface forming a feature such as a lake or wetland; however, in this case, upward vertical flow out of the top layer is effectively swept away. Fracture intensity and fracture transmissivity decrease with depth. The decrease is implemented by assigning different parameter values to each depth zone [11, Section 3.7].

II.B. Emplacement Concept and Repository Layout

The generic reference case uses the KBS-3V emplacement concept developed for the Swedish and Finnish repository programs [9] and adopted by several countries as the reference design for a generic reference case or in the preliminary stages of site investigation [3,4,13]. The KBS-3V concept is developed for a repository mined at a depth of approximately 500 m in sparsely fractured crystalline rock. Copper canisters, each containing a nominal inventory of 4 pressurized water reactor (PWR) assemblies, are emplaced within rings of

compacted bentonite in vertical deposition holes beneath the floor of a deposition tunnel, and tunnels are backfilled.

different depth zones, representing vertical variations within the subsurface. Each depth zone contains three different families, representing variations in orientation (strike and dip, or equivalently, trend and plunge) and

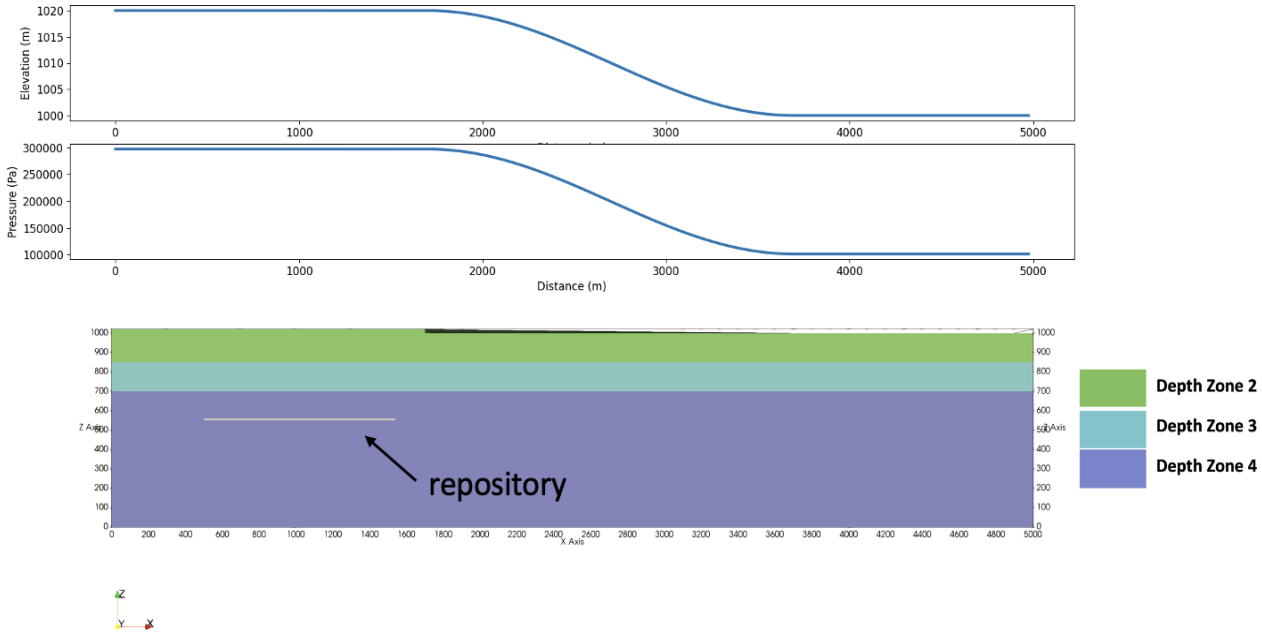

Fig. 1. Elevation profile and corresponding pressure boundary condition (top) and depth zones in the domain (bottom).

The waste inventory is 4,350 metric tons uranium (MTU) in the form of PWR SNF. Assuming each PWR assembly contains 0.435 MTU, 2500 4-PWR canisters are required to dispose of the inventory. The waste inventory is deliberately small to reduce the computational burden of simulations.

The repository, located at a depth of approximately 450 m, comprises 50 deposition drifts branching off two parallel access tunnels. The deposition drifts are spaced 40 m center-to-center; 50 deposition holes within each tunnel are spaced 6 m center-to-center. This spacing ensures that peak buffer temperatures do not exceed 100 ºC [9]. The deposition drifts are 306 m in length so that the deposition tunnel extends 6 m beyond the center of the last deposition hole at both ends. There are 50 individual deposition drifts which results in a total of 2,500 deposition boreholes.

II.C. Natural Barrier System

The crystalline host rock is characterized by occurrence of large-scale, highly fractured brittle deformation zones and intervening masses of competent rock containing sparse networks of connected fractures. Following the example of SKB [8], the former are named Hydraulic Conductor Domains (HCD) and the latter are named Hydraulic Rock Mass Domains (HRD). The fractures within the HRD are subdivided up into three hydraulic properties.

Conceptually, properties such as transmissivity of individual fractures exhibit a dependence on the present-day stress field. As a result, there is a greater density of fractures, larger proportion of subhorizontal fractures, and higher fracture transmissivity at shallower depths, and lower density of fractures, lower proportion of subhorizontal fractures, and lower fracture transmissivity at greater depths. The HCD are treated as deterministic features, i.e., their geometry and properties are the same in all realizations of reference case simulations. Fractures within the HRD are treated as stochastic features, i.e., multiple realizations of the fractured rock mass are generated by sampling probability distributions for fracture radius, fracture orientation, and fracture location.

II.D. Conservative Tracer Transport

In the first iteration of the reference case, teams are modeling steady state flow and conservative transport of two tracers. Tracer 1 and Tracer 2 are modeled after ^{129}I but they do not undergo radioactive decay. Both have an atomic weight of 128.9 g/mol. The total inventory of the two tracers in each waste package is 5.45 g (0.0423 moles), equivalent to 1/100th of the expected inventory of ^{129}I in a waste package containing 4 PWR assemblies. The inventory of Tracer 1 is 0.545 g (0.00423 moles), or 10%

of the total; it is instantly released at the start of the transport simulation. The inventory of Tracer 2 is 4.90 g (0.038 moles), or 90% of the total; it is released at a fractional rate of 10^{-7}/y throughout the transport simulation. It is assumed all canisters breach at the beginning of the simulation.

III. METHODS

III.A. Discrete Fracture Network Generation

Stochastic and deterministic fractures are generated using Los Alamos National Laboratory's (LANL) software dfnWorks [7]. dfnWorks takes inputs of probability distributions for fracture radius and orientation, and values for fracture density. Fracture transmissivity is a function of fracture radius. The reference case uses the fully-correlated relationship defined in [5]. Fracture aperture is calculated from the transmissivity using the cubic law [1]. The dfnWorks output must be post-processed to calculate depth dependent transmissivity, aperture, and permeability. Deterministic fractures are input by specifying normal vectors, radii, and translation from the origin. Stochastic fractures are randomly distributed in the domain until the target fracture density is reached. Isolated fractures and fracture clusters not connected to faces in the domain are discarded. Fracture apertures, permeabilities, normal vectors, and coordinates are output.

III.B. Equivalent Continuous Porous Medium

Fractures are upscaled using a Python script called mapdfn.py [10], which takes dfnWorks output and Equivalent Continuous Porous Medium (ECPM) model domain and discretization (origin, domain, length, and length of cubic grid cells) and outputs grid cell permeability, porosity, and tortuosity. Cell properties are calculated by determining the fractures that extend over the ECPM grid cell. For each fracture in a cell, intrinsic transmissivity (T_f[m^3]) is calculated as:

$$T_f = k_f b_f \#(1)$$

where k_f is fracture permeability [m^2] and b_f is fracture aperture [m]. Intrinsic transmissivity is described as a diagonal transmissivity tensor, where the coordinates are then rotated into the coordinates of the grid. Off-diagonal terms are discarded, and the diagonal tensor describe cell permeability is calculated as:

$$\begin{bmatrix} k_{xx} & & \\ & k_{yy} & \\ & & k_{zz} \end{bmatrix} = \frac{1}{d} \sum \begin{bmatrix} T_{xx} & & \\ & T_{yy} & \\ & & T_{zz} \end{bmatrix}_f \#(2)$$

where d is the length of the cell side, and the sum is over all fractures intersecting the cell. A stairstep correction is added to the permeability to account for the artificially low flux calculated from the ECPM due to fractures being characterized as staircases. The correction is derived from [12], where the amount of correction needed is determined by the dot product between each fracture in the grid cell and the normal vector to each coordinate axis and is applied based on the angle closest to 45°. Fracture porosity for each grid cell is calculated as:

$$\phi = \frac{1}{d} \sum b_f \#(3)$$

And cell tortuosity (τ) is calculated so the effective diffusion coefficient (D_e) is homogeneous everywhere in the fractured rock. In PFLOTRAN tortuosity is a number less than one so that:

$$D_e = \phi \tau D_m \#(4)$$

where D_m is the molecular diffusion coefficient in water. Cells not intersected by fractures are assigned matrix permeability and porosity. For the reference case, an upscaled grid cell size of 20 or 25 m is used (Fig. 2).

III.C. Model Domain

The mesh is created using Cubit [2] and formatted as an unstructured mesh that can be input into PFLOTRAN, a massively parallel flow and reactive transport simulator [6]. The deposition holes and waste packages are discretized to 25/27 or 20/27 m, the deposition drifts are discretized to 25/9 or 20/9 m, and the near field is discretized to 25/3 or 20/3 m. The fractures in the repository were then upscaled to a 25/3 or 20/3 m grid. The 20 m grid cell size results in closer sizing of the values specified in the Task Specification [11] for all repository parameters except for the volume of the canister. Therefore, both grid sizes are implemented and tested to see if the smaller volume of canister in the 20 m grid affects the transport results.

Steady state flow is implemented using PFLOTRAN Richards mode and transport is simulated using PFLOTRAN reactive transport mode. First a steady state flow solution is established using a constant pressure (Dirichlet) boundary condition at the top surface of the domain and no flow boundary conditions at all other faces of the domain. Then, transport of the two tracers is simulated for 100,000 years. The tracer advects out of the top boundary condition while no-flow boundary conditions are applied to all other faces. Initially the domain is empty of tracer everywhere except in the waste packages. The source terms for the tracers are simulated in PFLOTRAN using the Waste Form Process Model.

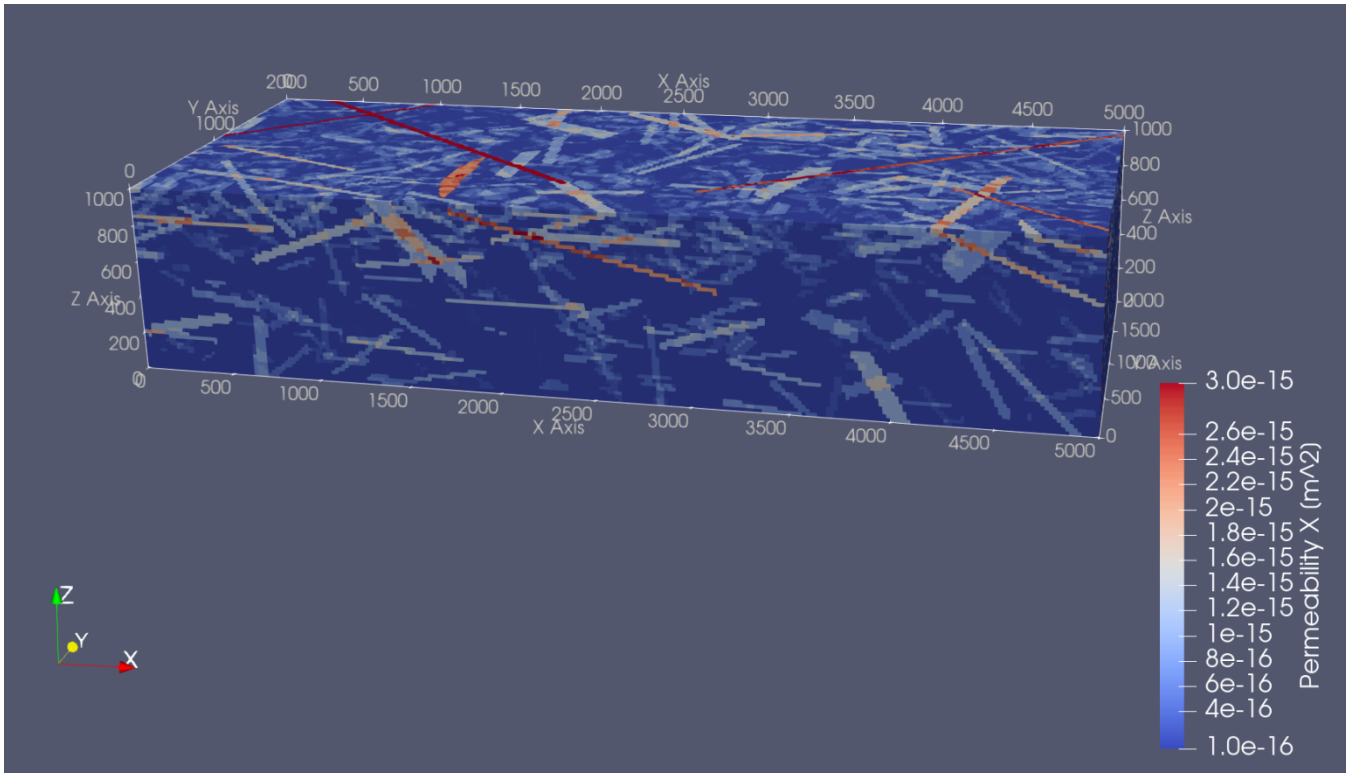

Fig. 2. Upscaled fracture domain using cell size of 20 m.

IV. OUTPUT METRICS

Three different surfaces of interest were defined at the top of the domain (z=1000 m). The surface of the high point (0 m < x < 1700 m), the surface of the hillslope (1700 m < x < 3700 m), and the surface of the low point (3700 m < x < 5000 m). The performance assessment results are then compared in the following ways: 1) steady state liquid flow across the high point, hillslope, and low point with time 2) tracer mass flow across the hillslope and low point with time, 3) largest tracer mass flow across the low point and hillslope and 4) tracer inventory remaining in the repository with time.

V. PRELIMINARY RESULTS

Figs. 3-12 show the preliminary results for the DOE team. The simulations were run on 8 nodes and 288 processors of a parallel super computer. The 20 m grid contains 3,454,936 total cells and the 25 m grid contains 2,051,032 total cells. The 25 m grid completed in ~10 minutes while the 20 m grid took ~496 minutes to complete. Both grid sizes were compared on Realization 1. Then, an initial test on the effect of the stochastic realizations on the outputs were run for each realization on the 25 m grid.

In Figs. 3 and 4 positive values represent outflow and negative values represent inflow of the steady state flow. Most of the tracer is exiting through the low point. The two grid sizes show good agreement with one another. Since simulation results on the two grids are similar, the faster 25 m grid simulations are used for comparison of the fracture network realizations. Fig. 4 shows the steady state fluxes for all realizations on the 25 m grid.

The tracer inventory remaining in the repository with time for Realization 1 is shown in Fig. 5. A large amount of Tracer 1 still remains in the repository at the end of the simulation. The calculation for total mass in the repository does not include the mass remaining in the waste package, which explains why Tracer 2 mass increases over time. Future work will include post processing the mass remaining in the waste package. Fig. 6 shows the mass remaining in the repository for all realizations in the 25 m grid. Tracer 2 behaves similarly for all realizations while Tracer 1 concentration shows increasing spread at later times.

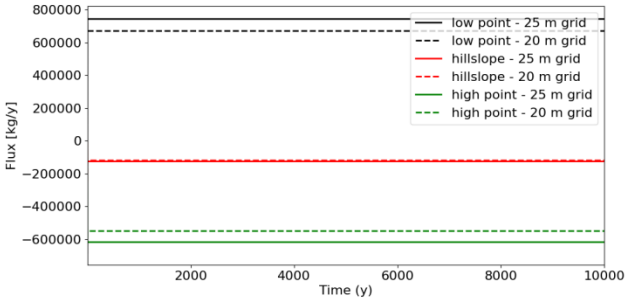

Fig. 3. Steady state flow for high point (green), hillslope (red), and low point (black) for 20 m grid (dashed) and 25 m grid (solid) on Realization 1.

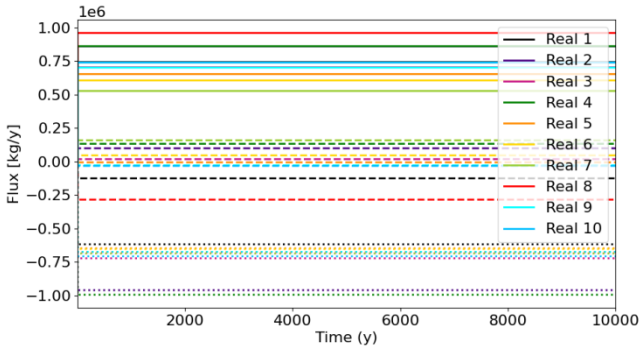

Fig. 4. Steady state flow for all realizations on the 25 m grid of high point (dotted), hillslope (dashed), and low point (solid).

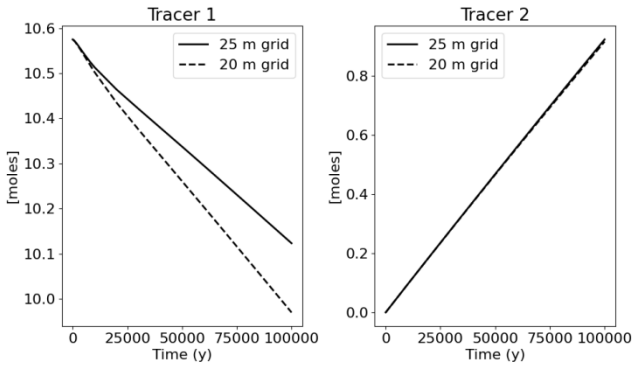

Fig. 5. Mass of Tracer 1 (left) and Tracer 2 (right) remaining in the repository on the 20 m grid (dashed) and 25 m grid (solid) on Realization 1.

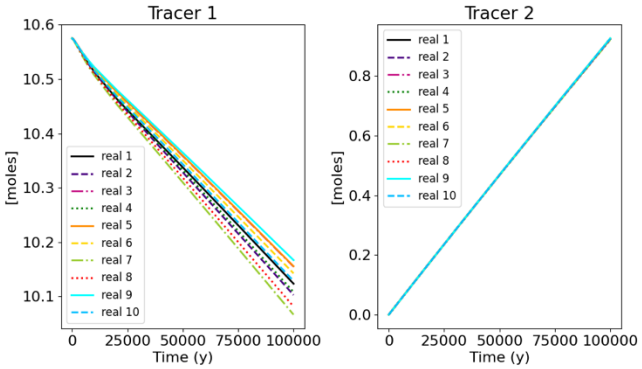

Fig. 6. Mass of Tracer 1 (left) and Tracer 2 (right) remaining in the repository for all realizations on the 25 m grid.

The cumulative mass flow (moles) and mass flow rate (moles/year) across the hillslope and the low point surface can be seen in Fig. 7 and Fig. 8 respectively. These values were calculated using the integral flux card in PFLOTRAN. The two grids are in good agreement with one another. The results for the hillslope and low point on all realizations for the 25 m grid can be seen in Fig. 9 and 10 respectively. Cumulative mass flow and mass flow over the hillslope and low point are highly dependent on the realization of the stochastic network.

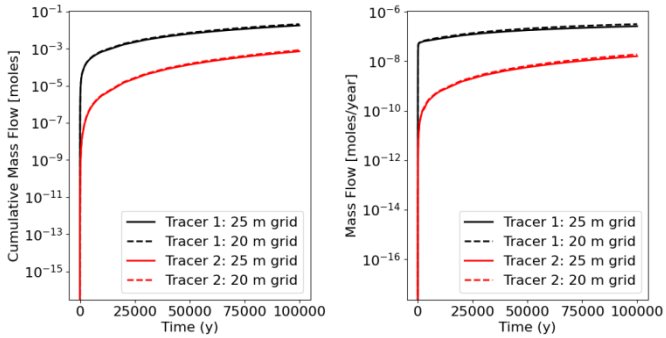

Fig. 7. Cumulative mass flow (left) and mass flow rate (right) across hillslope on Realization 1.

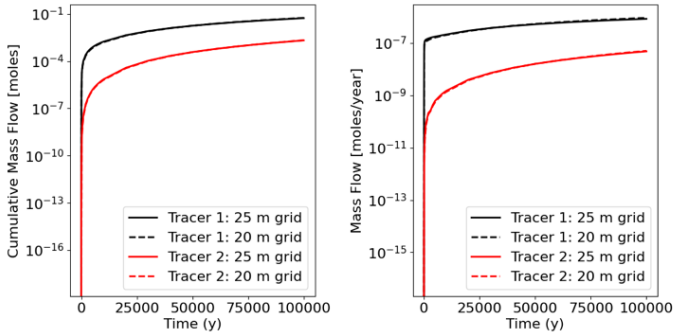

Fig. 8. Cumulative mass flow (left) and mass flow rate (right) across low point on Realization 1.

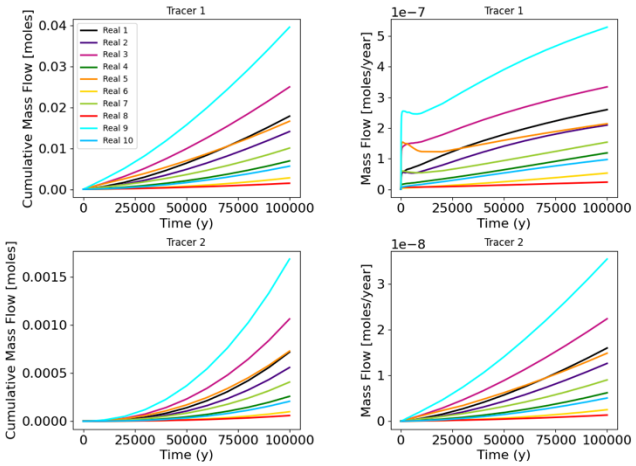

Fig. 9. Cumulative mass flow (left) and mass flow (right) across the hillslope for all realizations on the 25 m grid.

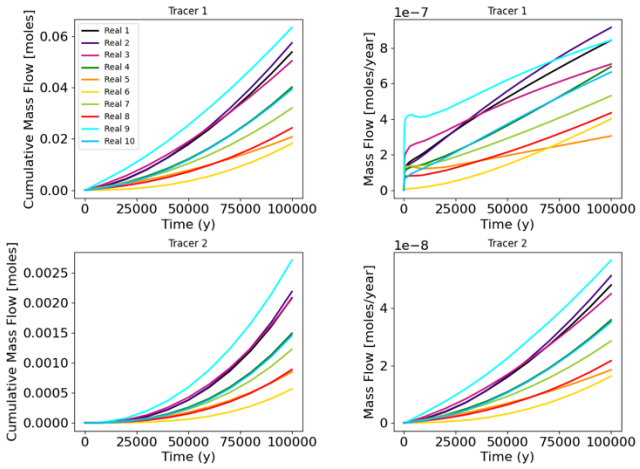

Fig. 10. Cumulative mass flow (left) and mass flow (right) across the low point for all realizations on the 25 m grid.

The cumulative mass flow over the area on the low point with the largest mass flow is shown in Fig. 11 for the 20 m grid and Fig. 12 for the 25 m grid on Realization 1. To calculate where the maximum mass flow occurred multiple integral flux cards were defined over each cell on the low point and then post processed to find the maximum mass flow. The largest mass flow occurs over areas where deterministic fractures intersect the top surface. For the 20 m grid the largest mass flow was at the grid cell covering 3880 m < x < 3900 m and 840 m < y < 860 m. For the 25 m grid the largest mass flow was found at the grid cell covering 3900 m < x < 3925 m and 750 m < y< 775 m. In order to make this calculation faster and more efficient, development work will be implemented in PFLOTRAN to calculate maximum mass flow over a surface inside the code and used to calculate the values for the hillslope and the remaining realizations.

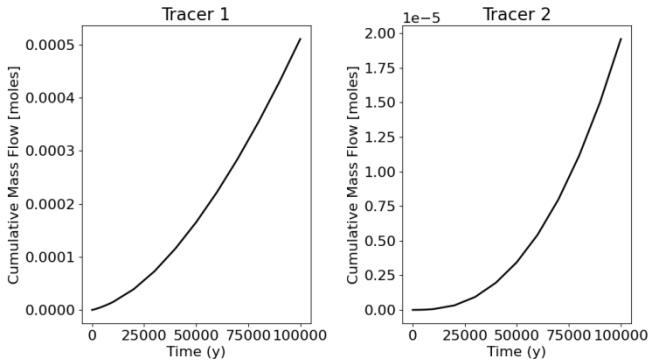

Fig. 11. Cumulative mass flow at the point on the low point where the maximum mass flow occurred on the 20 m grid in Realization 1.

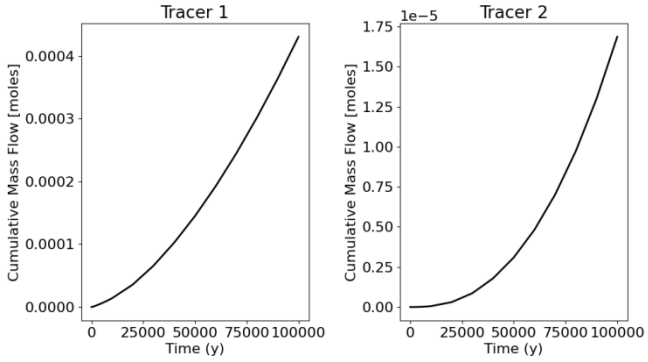

Fig. 12. Cumulative mass flow at the point on the low point where the maximum mass flow occurred on the 25 m grid in Realization 1.

VI. CONCLUSIONS

Task F1 of the DECOVALEX task is a comparison of performance assessment models in a generic mined repository in fractured crystalline rock. Preliminary modeling results from the DOE team for DECOVALEX Crystalline Task F1 are described in this paper. The DOE team is investigating two different grid cell sizes and currently working on calculating output metrics for all realizations, developing a more efficient method for calculating maximum mass flow across a surface, and comparing modeling results with other teams. A large fraction of Tracer 1 was still found in the repository at the end of the simulation and mass flow across surfaces of interests varied based on the stochastic fracture realization.

Complexity may be added to the reference case once the initial comparison is completed. This may include adding radionuclide source and ingrowth, decay, and sorption, matrix diffusion, and develop a canister breach

concept that results in transport on the highest-consequence paths identified through current modeling efforts. Future iterations may also explore uncertainty in a limited number of input parameters. This task will improve confidence in the methods used in performance assessment as well as identify areas in which more research is needed.

ACKNOWLEDGMENTS

Sandia National Laboratories is a multi-mission laboratory managed and operated by National Technology and Engineering Solutions of Sandia, LLC., a wholly owned subsidiary of Honeywell International, Inc., for the U.S. Department of Energy's National Nuclear Security Administration under contract DE-NA-0003525. SAND2022-XXXX.

REFERENCES

1. Bear K. 1993. *Flow and Contaminant Transport in Fractured Rocks,* Academic Press: 1-37
2. Blacker, T., S.J. Owen, M.L. Staten, R.W. Quador, B. Hanks, B. Clark, R.J. Meyers, C. Ernst, K. Merkley, R. Morris, C. McBride, C. Stimpson, M. Plooster and S. Showman (2016). *CUBIT Geometry and Mesh Generation Toolkit 15.2 User Documentation.* SAND2016-1649 R. Sandia National Laboratories, Albuquerque, New Mexico.
3. Choi, H. J., J. Y. Lee, and J. Choi 2013. "Development of Geological Disposal Systems for Spent Fuels and High-Level Radioactive Wastes in Korea". *Nuclear Engineering and Technology, 45*(1), 29-40. doi: 10.5516/net.06.2012.006
4. NWMO 2012. *Used Fuel Repository Conceptual Design and Postclosure Safety Assessment in Crystalline Rock*. NWMO TR-2012-16. Nuclear Waste Management Organization, Toronto, Ontario.
5. Follin, **S**., L. Hartley, P. Jackson, S. Joyce, D. Roberts, and B. Swift 2007. *Hydrogeological characterization and modeling of deformation zones and fracture domains, Forsmark modelling stage 2.2*. SKB R-07-48. Svensk Kärnbränslehantering AB, Stockholm, Sweden.
6. Hammond, G.E., Lichtner, P.C. and Mills, R.T. 2014. Evaluating the performance of parallel subsurface simulators: An illustrative example with PFLOTRAN. Water Resources Research, 50(1), 208-228. doi: 10.1002/2012wr013483
7. Hyman, J. D., S. Karra, N. Makedonska, C. W. Gable, S. L. Painter, and H. S. Viswanathan 2015. "DFNWORKS: A discrete fracture network framework for modeling subsurface flow and transport". *Computers & Geosciences*, 84, 10-19. doi: 10.1016/j.cageo.2015.08.001
8. Joyce,S., T. Simpson, L. Hartley, D. Applegate, J. Hoek, P. Jackson, D. Swan, N. Marsic, and S. Follin 2010. *Groundwater flow modelling of periods with temperate climate conditions - Forsmark*. SKB R-09-20. Svensk Kärnbränslehantering AB, Stockholm, Sweden.
9. Pettersson, S. and B. Lönnerberg 2008. 16-18 June 2008. *Final Repository for Spent Nuclear Fuel in Granite - The KBS-3V Concept in Sweden and Finland.* Paper presented at the International Conference Underground Disposal Unit Design & Emplacement Processes for a Deep Geological Repository, Prague.
10. Stein, E. R., J. M. Frederick, G. E. Hammond, K. L. Kuhlmann, P. E. Mariner, and S. D. Sevougian 2017. April 9-13, 2017. *Modeling Coupled Reactive Flow Processes in Fractured Crystalline Rock*. Paper presented at the International High-Level Radioactive Waste Management Conference, Charlotte, NC.
11. Stein, E.R., R. Jayne, T. LaForce, R. Leone, and S. Nguyen 2021. DECOVALEX-2023 Task F Specification, Revision 7. SAND2021-13423 O. Sandia National Laboratories, Albuquerque, New Mexico.
12. Sweeney, L. P., E. Basurto, D. M. Brooks, A.C. Eckert, P. E. Mariner, T. Portone, and E. R. Stein 2020. *Advances in Uncertainty Quantification and Sensitivity Analysis Methods and Applications in GDSA Framework*. SAND2020-10802 R. Sandia National Laboratories, Albuquerque, NM.
13. TPC (Taiwan Power Company) 2017. *The Technical Feasibility Assessment Report on Spent Nuclear Fuel Final Disposal*. Main Report. Taiwan Power Company, Taipei, Taiwan.